Adsorption of Gaseous Hydrocarbons on Activated Carbon: Characteristic Kinetic Curve

The internal diffusion coefficients, D_i, of pure methane, ethane and ethylene as well as some of their binary and ternary mixtures, have been calculated at 20°C for solid particles of a commercial activated carbon. It has been observed that the contribution of the surface migration mechanism to the global mass transfer process inside the adsorbent particles can be as much as 70–80%. Values for the surface migration coefficient D_s have also been calculated from the relation $D_i = D_g + KD_s$, where K is a dimensionless mean slope factor. Values found for both coefficients are of the same order of magnitude as those reported in the literature for similar systems.

All the values for the internal diffusion coefficients of these pure components and their mixtures fit into a single correlation curve, the characteristic kinetic curve of the adsorbent.

E. COSTA, G. CALLEJA and F. DOMINGO

Departamento de Ingeniería Química
Facultad de Ciencias Químicas
Universidad Complutense
Ciudad Universitaria,
Madrid, Spain

SCOPE

The increasing importance of adsorption processes for the separation of gaseous mixtures is due to the high selectivity and adsorption capacity of solid adsorbents, the less extreme operation conditions needed, and the small energy consumption required. Adsorption is becoming a competitive operation that can advantageously substitute for other separation operations such as distillation or liquid-liquid extraction. The advantages are especially attractive when the problem is the separation of light gases such as methane, ethane, ethylene and other typical hydrocarbons of gaseous refinery streams, since their separation by distillation requires expensive high pressure units.

Although there are some commercial processes for the separation of hydrocarbons using gas adsorption (Milton, 1963; Priegnitz, 1973; Yatsurugi, 1974; Broughton, 1977), the extension of this method to other cases of practical interest is generally limited by the lack of reliable fundamental data for estimating the feasibility of a given separation and for reducing the empiricism of the present design of adsorbers.

Among these fundamental data, the equilibrium adsorption isotherms and the internal diffusion coefficients of individual species of the mixture should be emphasized. Although substantial attention has been paid in the literature to the adsorption isotherms of pure compounds and their mixtures, even to the point of predicting multicomponent adsorption equilibria (Lewis et al., 1950; Myers and Prausnitz, 1965; Costa et al., 1981), most of the efforts on adsorption kinetics to calculate diffusion coefficients inside the porous particles of solid adsorbents and the contribution of different diffusion mechanisms (gas phase diffusion and surface migration) involved only pure components. However, kinetic data from mixtures for adsorption bed design are more useful than data from pure species. Data on diffusion coefficients of the individual components of a fluid mixture have been scarce up to now. Kokoszka (1970), Ma and Roux (1973) and Ma and Lee (1977) are among those who have shown that the adsorption rates of pure propane, *n*-butane, *i*-butane, 1-butene and other light gases into molecular sieves were lower when these compounds were present in binary mixtures. Feng et al. (1973, 1974) have extensively studied the diffusion of gaseous mixtures inside the pores of solid adsorbents, using several diffusion models. Their results, which were achieved by assuming a single pore size for the adsorbent and a reasonable tortuosity factor, were erroneous for not considering surface migration.

We present here new values for the internal diffusion coefficients of methane, ethane, and ethylene, both as pure components and as part of the mixtures of methane-ethylene, ethane-ethylene, and methane-ethane-ethylene, mixtures of evident practical interest for the purification of cracking gas streams, with activated carbon as the adsorbent, at temperature of 20°C, and hydrocarbon partial pressures up to 300 mm Hg (39.9 kPa).

The internal diffusion coefficients are calculated by comparing experimental kinetic curves with theoretical ones obtained from a mathematical model for diffusion and adsorption into the adsorbent pores. The model includes both diffusion mechanisms: gaseous phase diffusion into the pores of the adsorbent, and surface migration of adsorbed molecules.

CONCLUSIONS AND SIGNIFICANCE

The internal diffusion coefficient D_i and the surface migration coefficient D_s have been obtained from experimental data of adsorption for pure methane, ethane, and ethylene and various binary and ternary mixtures of the components in the range 0–300 mm Hg (0–39.9 kPa) hydrocarbon partial pressure and 20°C. The simple experimental technique uses a periodically fluidized bed of activated carbon and a mathematical model for adsorption that takes into account two possible mechanisms for the diffusion of the adsorbates into the adsorbent particles.

Values obtained for the internal diffusion coefficient D_i of pure hydrocarbons range from 2.10^{-4} to 5.10^{-3} cm²/s, increase in the order methane, ethylene, ethane for any given partial pressure, and decrease with increasing partial pressures. Values obtained for the surface migration coefficient D_s of pure hydrocarbons are about 10^{-6} cm²/s; they increase in the order ethane, ethylene, methane, and also slightly with progressive surface coverage.

With the exception of ethylene in its mixture with methane, the internal diffusion coefficients of the three individual hydrocarbons in their mixtures were always smaller than the coefficients of the pure components; they decreased with decreasing initial concentrations and with increasing partial pressures in the mixture. Under the experimental conditions investigated, the relative variations observed in all the internal diffusion coefficients were coincident with the variations of the slope of the respective equilibrium isotherms. This fact shows the close interrelation of these slopes, K, with the internal diffusion coefficients, D_i, according to the expression $D_i = D_g + KD_s$. Under these conditions, the contribution of the surface migration term KD_s to the global mass transfer inside the porous particles of the adsorbent is about 70–80%.

After plotting more than two hundred values of the internal diffusion coefficients of the three hydrocarbons, pure and mixed, against the mean values of the slope of their respective adsorption isotherms, a single curve was obtained with an average deviation of less than 5%. Since no precedent is known in the literature for such correlation, it has been called the "characteristic kinetic curve" of the adsorbent. Such a curve allows the determination of the internal diffusion coefficients of the mentioned hydrocarbons, as pure components or in their mixtures, from only the slope of the adsorption isotherms of the individual species, and could probably be extrapolated to conditions other than the ones investigated (e.g., different pressures, different mixtures, and even different temperatures).

THEORY

The gas adsorption rate is governed by three resistances in series:

a) Resistance to the adsorbate transfer through the external gas phase surrounding the adsorbent particles.

b) Resistance to the adsorbate diffusion through the pores of the solid particles.

c) Resistance corresponding to adsorption on the pore walls of the adsorbent.

The first of these resistances has been extensively studied, and thus several good correlations for calculating the corresponding mass transfer coefficient are available (Gamson, 1951). In addition, the first resistance for turbulent gas flow around the adsorbent usually is not significant. With respect to the third resistance, it is generally accepted that physical adsorption occurs almost instantaneously. Therefore, the global adsorption rate in this situation will be controlled by the second resistance, which can be characterized by an internal diffusion coefficient for each single adsorbate.

According to several investigators (Masamune and Smith, 1964; Chao and Hoelscher, 1966; Nemeth and Stuart, 1970; Costa et al. 1971, 1975), if each adsorbent particle is considered as a heterogeneous system formed by a porous solid phase and a gaseous phase filling the void fraction of the solid, the internal diffusion coefficient D_i can be expressed in terms of two other diffusion coefficients that characterize the two possible simultaneous mechanisms of diffusion: (a) A molecular or Knudsen diffusion coefficient for the adsorbate molecules diffusing through the gas filling the pores, D_g, and (b) a surface migration coefficient for the adsorbed molecules moving along the solid surface, D_s. Thus, for linear adsorption isotherms, the total flux of adsorbate into the solid adsorbent could be expressed by Fick's law of diffusion using a global internal diffusion coefficient represented by an equation similar to that used by Masamune and Smith (1964):

$$D_i = D_g + KD_s \tag{1}$$

where K represents a dimensionless mean slope of the equilibrium isotherm in the concentration range of each experiment.

Other authors (Meyer and Weber, 1967; Lee and Weber, 1969; Marcussen, 1970; Lee and Chi, 1971; Furusawa and Smith, 1973) have developed this pore diffusion model for nonlinear adsorption isotherms, assuming spherical shape for the adsorbent particles and using analytical or numerical integration techniques.

However, there are no general correlations available to estimate these global internal diffusion coefficients for pure and mixed hydrocarbons, as previously indicated. Therefore, the practical interest of theoretical models to predict the breakthrough curves of fixed bed adsorption columns is notably limited.

In this paper we present new experimental data of internal diffusion coefficients of pure methane, ethane, and ethylene, and their binary and ternary mixtures of various compositions.

MATHEMATICAL MODEL

The mathematical model used to calculate the internal diffusion coefficients from the experimental measurements of time dependent concentrations of diffusing species takes into account the two stated possible simultaneous mechanisms: gas phase diffusion and surface migration of adsorbed molecules. This previously used model (Costa et al., 1971, 1975) is based on the following transport equations for each adsorbate inside the pores:

Gaseous phase: $$\frac{\partial c_g}{\partial t} = D_g \nabla^2 c_g + R_g \tag{2}$$

Adsorbed phase: $$\frac{\partial c_s}{\partial t} = D_s \nabla^2 c_s + R_s \tag{3}$$

where c_g and c_s are molar concentrations of the adsorbate in the gaseous and solid phases of the adsorbent, respectively, and R_g and R_s are the corresponding generation terms. The two generation terms are interrelated by Eq. 4, and the concentrations c_g and c_s are related by the adsorption isotherm, Eq. 5:

$$-R_s = \left(\frac{\alpha_p}{1-\alpha_p}\right) R_g \tag{4}$$

$$dc_s = \left(\frac{\alpha_p}{1-\alpha_p}\right) K dc_g \tag{5}$$

Equations 2 and 3 can be rewritten into a single equation in terms of the gaseous concentration of the adsorbate in the pores:

$$\frac{\partial c_g}{\partial t} = \frac{D_i}{1+K} \nabla^2 c_g \tag{6}$$

where D_i represents the internal diffusion coefficient, expressed by Eq. 1.

Assuming that the actual cylindrical particles of the active carbon used can be represented by spheres of equal relation (external surface/volume) to obtain a simple analytical solution (it was experimentally observed that this simplifying hypothesis was acceptable by Costa et al., 1975), Eq. 6 takes the following form in spherical coordinates:

$$\frac{\partial c_g}{\partial t} = \frac{D_i}{1+K}\left(\frac{\partial^2 c_g}{\partial r^2} + \frac{2}{r}\frac{\partial c_g}{\partial r}\right) \tag{7}$$

On the other hand, a macroscopic balance for the adsorbate in the external gas mixture surrounding the adsorbent particles can be expressed in our case by the following equation:

$$\frac{dC}{dt} = -\frac{3W\alpha_p}{V\rho_p r_o} D_i \left(\frac{\partial c_g}{\partial r}\right)_{r=r_o} \tag{8}$$

Equations 7 and 8 can be integrated with the following initial and boundary conditions:

$$t = 0, \quad C = C_o, \quad c_g = c_{g_o}, \quad c_s = c_{s_o} \tag{9}$$

$$t > 0 \quad r = r_o \quad C = C_s \tag{10}$$

$$t > 0 \quad r = 0 \quad \left(\frac{\partial c_g}{\partial r}\right)_{r=0} = 0 \tag{11}$$

The boundary condition expressed in Eq. 10 holds when the external resistance to the adsorbate transfer through the gas film surrounding the particles is not significant. This was the case under our experimental conditions, since the results of the model were not at all affected by very large variations of the mass transfer coefficient through the gas film (k_g), using Gamson's (1951) correlation to calculate it, with a boundary condition that equals the molar flux through the gas film (in terms of k_g) and the molar flux of diffusion into pores of the particles. This model was solved analytically in a previous work by Costa et al. (1971), following the method recommended by Edeskuty and Amundson (1952), to give a dimensionless concentration of the adsorbate in the bulk gas around the particles as a function of time:

$$Y = \frac{C - c_{g_o}}{C_o - c_{g_o}} = Y_e + 6\epsilon \sum_{n=1}^{\infty} \frac{(\gamma_n \cos\gamma_n - \sin\gamma_n)\exp[-\gamma_n^2 t/\beta r_o^2]}{\gamma_n^2[\gamma_n \cos\gamma_n + (3\epsilon + 2)\sin\gamma_n]} \tag{12}$$

where:

$$\epsilon = (1+K)\frac{W\alpha_p}{V\rho_p}, \quad \beta = (1+K)/D_i \tag{13}$$

and γ_n are the successive solutions of the transcendental equation:

$$\frac{\tan\gamma}{\gamma} = \frac{3\epsilon}{\gamma^2 + 3\epsilon} \tag{14}$$

The term Y_e in Eq. 12 represents the equilibrium dimensionless concentration of the adsorbate in the bulk gas phase for $C = C_e$ that was also experimentally obtained, as shown later.

Under our experimental conditions it is reasonable to assume that diffusion through the gas filling the pores is a Knudsen diffusion. Furthermore, for the term representing the surface migration contribution KD_s (Eq. 1), the differences between the values of K for a component in the pure state and in a mixture are much more important than the corresponding differences of D_s. This is particularly true for the low concentration range, that is, far from saturation, where values of K are very high. Under these circumstances, the application of the established mathematical model to a mixture of adsorbates leads to an expression identical to Eq. 12 for each of the adsorbates.

Obtaining the Internal Diffusion Coefficients

With assigned numerical values for D_i, Eq. 12 allows calculation of the dimensionless concentration Y as a function of time, and so yields a theoretical curve $Y(t)$ for any assumed internal diffusion coefficient. A group of such theoretical curves can be compared with the experimental one to deduce the value of D_i for each adsorbate. The comparison was made in the following way: For each set of theoretical curves the assumed internal diffusion coefficient D_i and the calculated equilibrium time t_e (for which each curve became practically horizontal) was correlated with

$$D_i = a t_e^{\,b} \tag{15}$$

and the two empirical parameters, a and b, were determined by linear regression analysis. The equilibrium time, t_e, was established in each case by assuming a theoretical value for the dimensionless concentration Y separated from the equilibrium experimental value $(Y_e)_{\text{exp}}$ (for $C = (C_e)_{\text{exp}}$ in Eq. 12), by less than 0.0003, a difference that implies an error of less than 0.3%.

Finally, the experimental value for D_i was easily deduced in each case by using the experimentally determined value of t_e in Eq. 15. A sample calculation for one experiment has been included in the Appendix.

The convergence of the series in Eq. 12 was relatively slow, especially for the highest values of D_i, but in all cases the number of terms under the summation grouping required for an accurate calculation of t_e was smaller than 300, the limiting number of terms set in the calculation program.

EXPERIMENTAL

The experimental system was essentially the same used previously and has been already described (Costa et al., 1981). It consists basically of a

TABLE 1. PHYSICAL PROPERTIES AND CHARACTERISTICS OF ADSORBENT*

Carbon type	AC-40, cylindrical
BET surface area, m^2/g	782
Particle porosity	0.715
Real density, g/cm^3	3.06
Particle radius, cm	0.081
Particle length, cm	0.302
Adsorbent bed diameter, cm	5.1
Adsorbent bed static height, cm	5.0
Weight of adsorbent in bed, g	54

* Activated carbon AC-40, from CECA, S.A., Spain.

TABLE 2. INTERNAL DIFFUSION COEFFICIENT OF PURE HYDROCARBONS IN ACTIVATED CARBON AT 20°C

Experiment	a	b	t_e (min)	$\overline{P}$ (mm Hg)	$\overline{N}$ (mol/g)	K^*	D_i (cm^2/s)
				Methane			
1	0.18398	−0.91000	8	1.44	$4.50\ 10^{-6}$	174.80	0.00067
2	0.27300	−1.00000	6	4.58	$1.32\ 10^{-5}$	139.93	0.00076
3	0.28220	−1.02215	6	9.57	$2.48\ 10^{-5}$	124.55	0.00069
4	0.28265	−1.03734	6	17.65	$4.13\ 10^{-5}$	106.79	0.00063
5	0.18573	−0.98682	8	28.50	$6.10\ 10^{-5}$	96.62	0.00042
6	0.20307	−1.01114	8	67.52	$1.23\ 10^{-4}$	89.36	0.00039
7	0.09303	−0.89003	8	101.80	$1.76\ 10^{-4}$	84.55	0.00038
8	0.16560	−1.00000	6	145.76	$2.39\ 10^{-4}$	74.71	0.00046
				Ethane			
1	2.69996	−1.00000	8	0.50	$3.42\ 10^{-5}$	3,213.28	0.00562
2	2.21189	−0.98879	8	1.29	$7.53\ 10^{-5}$	2,730.53	0.00494
3	2.03997	−1.00000	8	2.39	$1.23\ 10^{-4}$	2,201.28	0.00425
4	1.88545	−1.01207	6	4.01	$1.80\ 10^{-4}$	1,794.60	0.00488
5	1.48780	−1.00559	8	6.30	$2.44\ 10^{-4}$	1,393.58	0.00299
6	1.15199	−1.00000	8	10.04	$3.22\ 10^{-4}$	1,031.71	0.00240
7	1.11774	−1.01468	10	16.36	$4.27\ 10^{-4}$	868.76	0.00170
8	0.81948	−1.00197	8	36.88	$6.85\ 10^{-4}$	629.01	0.00169
9	0.41945	−0.92998	8	53.86	$8.47\ 10^{-4}$	459.00	0.00135
				Ethylene			
1	2.80957	−0.99869	8	0.14	$8.37\ 10^{-6}$	3,462.17	0.00590
2	2.48003	−1.00429	8	0.44	$2.51\ 10^{-5}$	2,741.16	0.00503
3	2.36053	−1.00424	8	0.92	$4.78\ 10^{-5}$	2,554.28	0.00479
4	1.71322	−0.99511	8	1.78	$8.27\ 10^{-5}$	1,717.84	0.00368
5	1.53082	−1.00986	8	3.74	$1.35\ 10^{-4}$	1,363.39	0.00300
6	1.10246	−0.99999	8	8.81	$2.26\ 10^{-4}$	915.49	0.00230
7	0.77713	−0.99516	8	20.12	$3.70\ 10^{-4}$	609.54	0.00167
8	0.72652	−1.00770	8	41.72	$5.53\ 10^{-4}$	400.08	0.00144
9	0.51822	−1.00770	10	80.23	$7.92\ 10^{-4}$	315.76	0.00082
10	0.38120	−0.99946	6	124.57	$1.01\ 10^{-3}$	232.60	0.00106

SI conversion: mm Hg × 0.133 = kPa.

periodically fluidized bed of adsorbent, a membrane compressor for circulating the gaseous mixture through the bed, and a gas chromatograph for the analysis of the gas phase.

The hydrocarbons were supplied by the Sociedad Española del Oxígeno, S.A. (SEO, S.A.) with the following minimum purity grades: methane, 99.95%; ethane, 99.0%; and ethylene, 99.93%. Helium was also supplied as inert gas with a minimum purity of 99.998%.

The physical properties and characteristics of the adsorbent used, an activated carbon supplied by Compañía Española de Carbones Activos, S.A. (CECA, S.A.), are summarized in Table 1.

The experimental procedure was analogous to that used to obtain the equilibrium isotherms of hydrocarbon gas mixtures (Costa et al., 1981). In the present study, the gaseous phase was periodically analyzed by gas chromatography during each experiment, recording values of the concentration of each adsorbate and the total pressure with time, until equilibrium was attained. These experiments, repeated with ever-increasing initial compositions of the gaseous mixture, covered the entire concentration range in each adsorption isotherm. The successive amounts of adsorbate added were always small enough to consider the adsorption isotherm to be linear in the composition range of each experiment. The amounts adsorbed were always calculated from mass balances.

All the experiments were conducted at 20°C, with partial pressures for the adsorbates in the range of 0–300 mm Hg (0–39.9 kPa). The experiments with hydrocarbon mixtures were extended to several initial compositions of the gas mixture. Under these experimental conditions, adsorption of helium was negligible.

RESULTS AND DISCUSSION

Pure Hydrocarbons

Table 2 summarizes the results of a series of experiments to determine the internal diffusion coefficient D_i for the three pure hydrocarbons. Each experiment has been characterized by an average partial pressure $\overline{P}$ and adsorbed concentration $\overline{N}$, representative of the average equilibrium conditions corresponding to the short segment of the isotherm implied in each run. Table 3 gives the isothermal equilibrium data of the three pure hydrocarbons.

Figure 1 represents the internal diffusion coefficients of Table 2 vs. the square root of partial pressures, for each pure hydrocarbon. For a given adsorbate the internal diffusion coefficient decreases as its partial pressure increases, and for any given partial pressure the coefficient increases in the order: methane, ethylene, ethane. These variations can be easily understood considering the experimental adsorption isotherms of the pure hydrocarbons represented in Table 2. Since for the considered partial pressures, the values of D_g and D_s are not very different for the three hydrocarbons, and since the equilibrium isotherm slope K for methane is lower than those for the other hydrocarbons, Eq. 1 dictates that the surface migration term KD_s will be lower, and hence D_i will be lower, than those for the other hydrocarbons.

Figures 2–4 represent the internal diffusion coefficients vs. the average slope of the adsorption isotherm. The internal diffusion coefficient of each pure hydrocarbon results in a practically linear function of the average slope of their respective adsorption isotherms in the concentration range investigated. Therefore, according to Eq. 1, the slope of each straight line in Figures 2–4 will represent the average value of the surface migration coefficient D_s for each pure hydrocarbon. Table 4 summarizes these average values and the intervals of the isotherm slope K and partial pressure P for which they are valid.

It is evident that the internal diffusion coefficient of each component is highly sensitive to the slope of its adsorption isotherm. That means that the *contribution of surface migration is very im-*

Table 3. Adsorption Isotherms on Activated Carbon at 20°C of Pure Hydrocarbons, Binary Mixtures, and Ternary Mixtures

Pure Hydrocarbons

Methane		Ethane		Ethylene	
P (mm Hg)	*N* (mol/g)	*P* (mm Hg)	*N* (mol/g)	*P* (mm Hg)	*N* (mol/g)
2.88	9.010 10^{-6}	0.21	1.722 10^{-5}	0.27	1.673 10^{-5}
6.27	1.750 10^{-5}	0.80	5.115 10^{-5}	0.61	3.341 10^{-5}
12.86	3.219 10^{-5}	1.79	9.953 10^{-5}	1.24	6.221 10^{-5}
22.44	5.050 10^{-5}	3.00	1.472 10^{-4}	2.32	1.031 10^{-4}
34.55	7.144 10^{-5}	5.03	2.124 10^{-4}	5.15	1.661 10^{-4}
52.67	9.950 10^{-5}	7.58	2.760 10^{-4}	12.48	2.862 10^{-4}
82.37	1.470 10^{-4}	12.53	3.674 10^{-4}	27.77	4.530 10^{-4}
121.23	2.058 10^{-4}	20.19	4.865 10^{-4}	55.66	6.527 10^{-4}
170.29	2.714 10^{-4}	29.41	6.012 10^{-4}	104.80	9.304 10^{-4}
		44.36	7.695 10^{-4}	144.34	1.095 10^{-3}
		63.35	9.255 10^{-4}		

C_2H_4 in binary mixtures (C_2H_4 + C_2H_6)

I.V.R. = 8.5/1.5**		1/1		1.5/8.5	
P (mm Hg)	*N* (mol/g)	*P* (mm Hg)	*N* (mol/g)	*P* (mm Hg)	*N* (mol/g)
1.07	5.736 10^{-5}	0.71	3.341 10^{-5}	0.25	9.791 10^{-6}
2.77	1.130 10^{-4}	2.25	7.859 10^{-5}	1.03	2.893 10^{-5}
7.65	2.195 10^{-4}	4.20	1.153 10^{-4}	2.66	5.618 10^{-5}
14.55	3.196 10^{-4}	6.33	1.444 10^{-4}	5.17	8.064 10^{-5}
23.15	4.146 10^{-4}	11.21	2.018 10^{-4}	9.60	1.106 10^{-4}
37.82	5.521 10^{-4}	21.00	2.788 10^{-4}	14.70	1.382 10^{-4}
56.36	6.779 10^{-4}	36.90	3.716 10^{-4}	21.96	1.700 10^{-4}
81.10	8.454 10^{-4}	56.36	4.549 10^{-4}	33.20	2.080 10^{-4}
105.15	1.015 10^{-3}			47.87	2.535 10^{-4}

C_2H_4 in ternary mixtures (CH_4 + C_2H_6 + C_2H_4)

I.V.R. = 3/2/1**		1/2/2		3/1/1		1/1/2		3/1/2	
P (mm Hg)	*N* (mol/g)	*P* (mm Hg)	*N* (mol/g)	*P* (mm Hg)	*N* (mol/g)	*P* (mm Hg)	*N* (mol/g)	*P* (mm Hg)	*N* (mol/g)
0.45	1.973 10^{-5}	1.51	6.671 10^{-5}	0.27	1.353 10^{-5}	0.95	4.681 10^{-5}	0.85	3.999 10^{-5}
1.49	5.223 10^{-5}	4.66	1.288 10^{-4}	1.01	3.990 10^{-5}	4.45	1.348 10^{-4}	2.07	7.896 10^{-5}
4.00	9.811 10^{-5}	13.98	2.437 10^{-4}	2.83	8.885 10^{-5}	13.77	2.512 10^{-4}	5.82	1.531 10^{-4}
7.55	1.415 10^{-5}	26.34	8.425 10^{-4}	7.96	1.666 10^{-4}	37.69	4.598 10^{-4}	17.32	2.890 10^{-4}
		41.53	4.465 10^{-4}	14.90	2.391 10^{-4}	69.60	6.473 10^{-4}		
		69.95	5.760 10^{-4}	24.73	3.241 10^{-4}	102.01	8.324 10^{-4}		
				36.24	4.040 10^{-4}				

SI Conversion: mm Hg × 0.133 = kPa.

** Initial Volumetric Ratio of C_2H_4/C_2H_6 in binary mixtures and $CH_4/C_2H_6/C_2H_4$ in ternary mixtures.

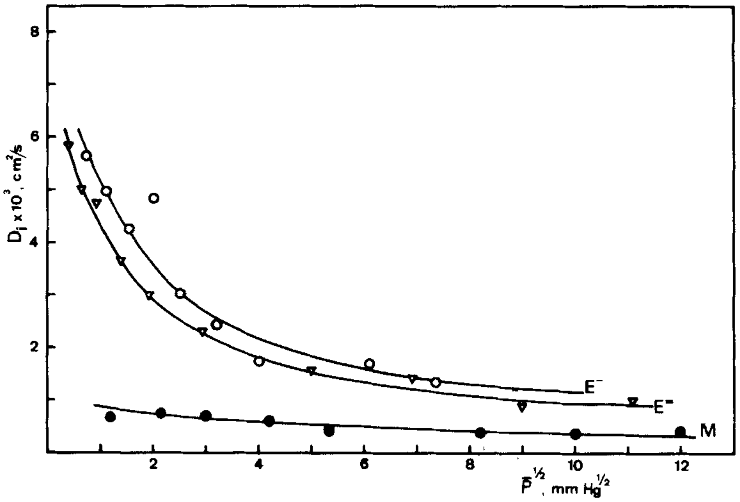

Figure 1. Adsorption of pure hydrocarbons: methane (M), ethane (E^-) and ethylene ($E^=$) on activated carbon at 20°C. Internal diffusion coefficients as a function of partial pressure of adsorbate.

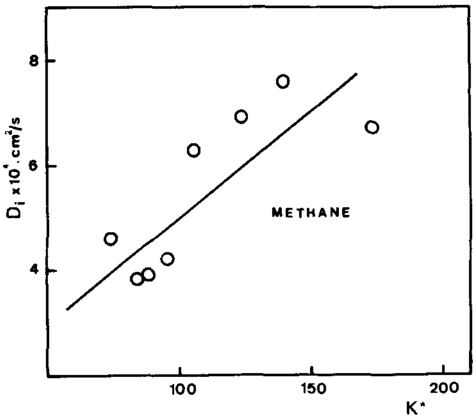

Figure 2. Variation of the internal diffusion coefficient of methane (D_i) with the slope of its equilibrium isotherm (K^*) at 20°C.

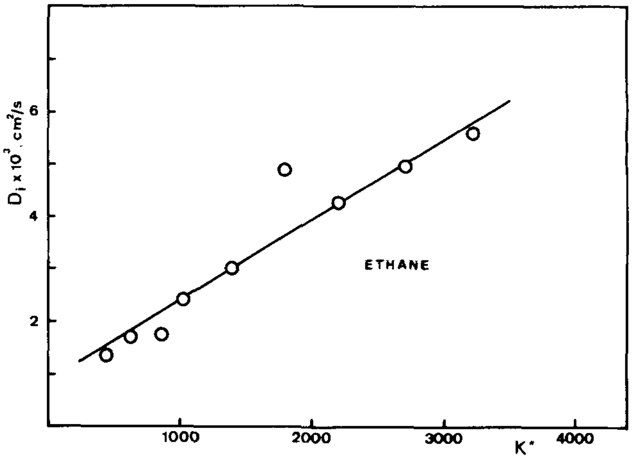

Figure 4. Variation of the internal diffusion coefficient of ethane (D_i) with the slope of its equilibrium isotherm (K^*) at 20°C.

portant in spite of the low values of the surface migration coefficient itself. These results are in agreement with others in the literature (Masamune and Smith, 1964; Schneider and Smith, 1968; Gilliland et al., 1974; Sladek et al., 1974).

On the other hand, it is obvious in the case of the hydrocarbons investigated that the surface migration coefficient is inversely related to the retention time of the molecules of the solid surface. Since the energy required for adsorbed molecules to leave the surface before being readsorbed is directly related to the adsorption energy (Smith, 1980), a higher adsorption capacity for a given adsorbate will mean a higher adsorption energy. This will result in a long retention time, and therefore a lower surface migration coefficient. So, the higher adsorption capacity of ethane and ethylene with respect to methane explains the lower values of the surface migration coefficients found for the two first hydrocarbons, as shown in Table 4.

Binary Mixtures

Two mixtures, methane-ethylene and ethane-ethylene, have been investigated. Figure 5 shows the internal diffusion coefficients of ethylene as a pure component and of ethylene as a component in three different initial ethylene-ethane compositions. Table 3 summarizes the individual adsorption isotherms of ethylene in the binary ethane-ethylene mixtures shown in Figure 5.

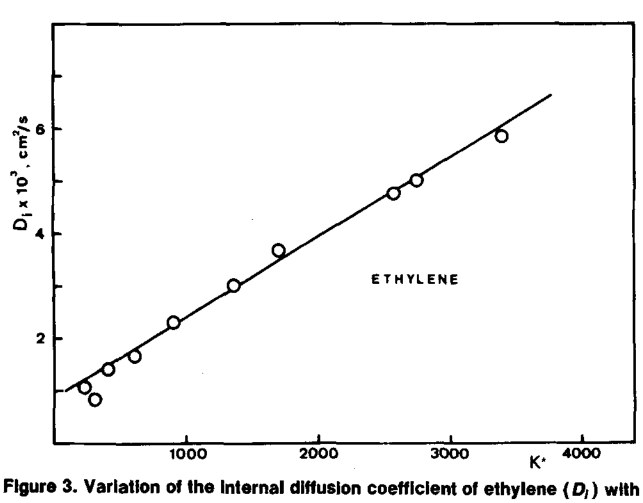

Figure 3. Variation of the internal diffusion coefficient of ethylene (D_i) with the slope of its equilibrium isotherm (K^*) at 20°C.

In Figure 5 it is observed that internal diffusion coefficients of ethylene in the presence of ethane are always smaller than those of pure ethylene, decreasing with its initial concentration in the mixture and with its increasing partial pressure. These variations of the internal diffusion coefficients are parallel to the variations observed in the slopes of the respective adsorption isotherms, Table 3, from which the important contribution of the surface migration term KD_s to the global diffusion coefficient D_i is confirmed.

When investigating the diffusion of ethylene in the binary mixture ethylene-methane (Domingo, 1981), it was observed that the internal diffusion coefficients of ethylene are not influenced by the presence of methane. This can be explained by the large difference in adsorption capacity of methane and ethylene on activated carbon at 20°C. Accordingly, since the adsorption capacities of ethane and ethylene are more similar, it is not surprising that a competitive diffusion of the two hydrocarbons will occur, resulting in lower values for the internal diffusion coefficient of each hydrocarbon. This can be observed in Figure 5 for ethylene.

Ternary Mixtures

Just as in the case of binary mixtures, Figure 6 represents the internal diffusion coefficients of ethylene in its ternary mixture methane-ethane-ethylene vs. the square root of the average partial pressure in each experiment, for the initial compositions of six different mixtures. Table 3 shows the individual adsorption isotherms of ethylene in the same ternary mixtures of methane, ethane, and ethylene represented in Figure 6. The results are similar to those obtained for binary mixtures, showing that the internal diffusion coefficients of each individual hydrocarbon in the ternary mixture are always smaller than the corresponding internal diffusion coefficients of the pure species under the same conditions.

TABLE 4. AVERAGE SURFACE DIFFUSION COEFFICIENT OF PURE HYDROCARBONS ON ACTIVATED CARBON AT 20°C

Adsorbate	D_s (cm^2/s)	K^* Range	P Range (mm Hg)
Methane	9.1 10^{-6}	175–70	0–170
Ethylene	3.9 10^{-6}	3,400–230	0–140
Ethane	3.8 10^{-6}	3,200–320	0–120

SI Conversion: kPa = mm Hg × 0.133.

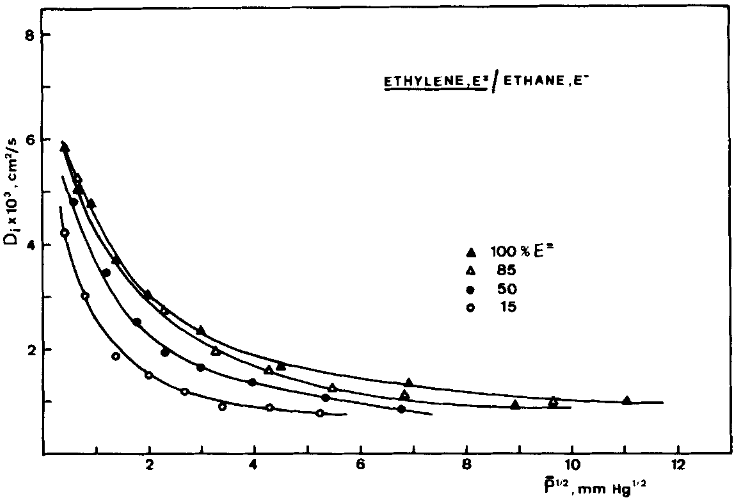

Figure 5. Adsorption of binary mixture ethane (E^-)/ethylene ($E^=$) on activated carbon at 20°C. Effect of mixture initial composition and average partial pressure of ethylene on the internal diffusion coefficient of ethylene.

It can be seen in Figure 6 that the presence of methane exerts only a slight influence on the internal diffusion coefficient of ethylene, due to the higher adsorption capacity of the latter hydrocarbon, and that the initial ethane/ethylene proportion has a strong effect on this diffusion coefficient. This is more clearly observed in Figure 7, where the internal diffusion coefficients of ethane and ethylene are plotted again for only the binary and ternary mixtures that have the same ethane/ethylene relation (1:1), giving just two curves, one for each hydrocarbon, regardless of the presence and initial proportion of methane.

CHARACTERISTIC KINETIC CURVE

When plotting the 210 values of the internal diffusion coefficient of the three hydrocarbons, both as pure components and as components in their binary and ternary mixtures, against the corresponding mean slopes of their respective individual adsorption isotherms, only a single curve is obtained (Figure 8), characteristic of the diffusion rate of these hydrocarbons into the activated carbon at 20°C. No precedent for such a curve is known in the literature.

According to Eq. 1, the slope of the characteristic kinetic curve of the adsorbent at each point in Figure 8 represents the surface migration coefficient D_S. This curve has been fitted by a polynomial function and its slope, mathematically calculated. Thus, D_s is represented vs. the isotherm slope K^*, Figure 9. It is now clearly shown that a sharp initial decrease of the surface migration coefficient with the slope K^* for low values of this parameter ($K^* \lesssim 200$) is followed by a more gradual decrease of D_S. For the range of high values of K^* ($K^* \gtrsim 200$), the surface diffusion coefficients show a relatively small continuous increase with progressive surface coverage (decreasing K^*). Since this range corresponds only to experimental points of ethane and ethylene, and the difference in their respective average surface migration coefficients is only about 2%, it can be concluded that the increase of the surface migration

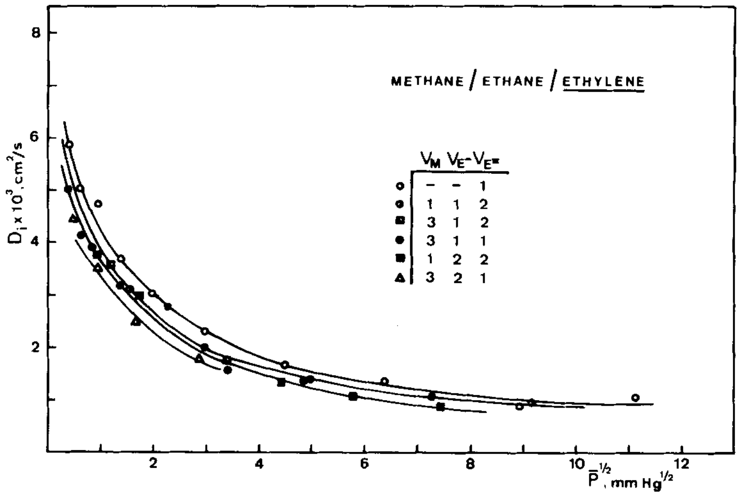

Figure 6. Adsorption of ternary mixture methane (M)/ethane (E^-)/ethylene ($E^=$) on activated carbon at 20°C. Effect of mixture initial composition and average partial pressure of ethylene on its individual internal diffusion coefficient.

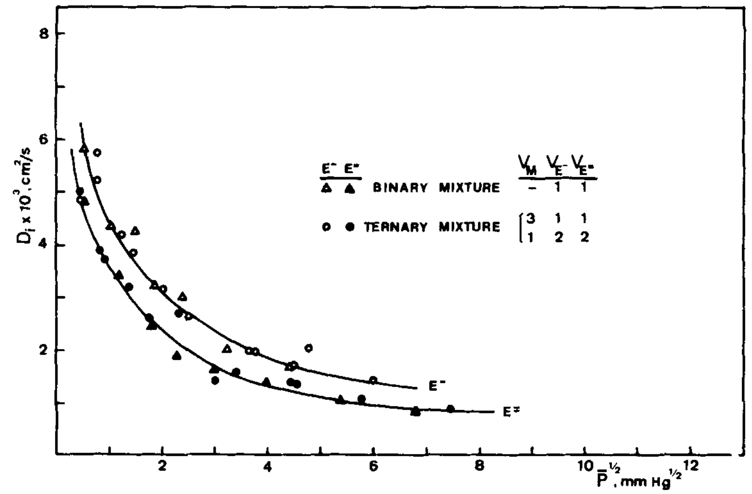

Figure 7. Individual internal diffusion coefficients of ethane (E⁻)(△) and ethylene (E⁼)(▲) in their binary mixture 1:1 and of ethane (E⁻)(○) and ethylene (E⁼)(●) in their ternary mixtures 3:1:1 and 1:2:2.

coefficient with progressive surface coverage in the range studied is probably due to the advantageous effect of the increasing repulsion of adsorbed molecules, which is in agreement with the conclusions of other authors (Gilliland et al., 1958, 1974; Ponzi et al., 1977; Sudo et al., 1978). On the other hand, the sharp increase of the surface migration coefficient for values of the slope K^* lower than 200 can be explained by taking into account that this range of slopes corresponds only to adsorbates of low adsorption capacity, such as methane in our case, which has a much higher surface diffusion coefficient than ethane and ethylene (Table 4). The average surface migration coefficient of methane indicated in Table 4 is in fact an average value of the corresponding range in the curve of Figure 9.

From this curve and the characteristic kinetic curve (Figure 8), Eq. 1 allows the evaluation of D_g for each component (Domingo, 1981). Comparison of these values with those expected from the Knudsen diffusivity, yielded tortuosity factors of 4 to 6, which are of the same order of magnitude of those reported by others (Smith, 1981). These tortuosity factors were found to increase slightly with pressure.

Finally, Figure 10 clearly shows the contribution of the surface migration mechanism to the global mass transfer process inside the adsorbent particles expressed as $(KD_s/D_i)\cdot 100$ versus the slope K^*. It can be observed that the contribution of KD_s is as much as 70–80% for practically the whole range of slopes of the adsorption isotherms.

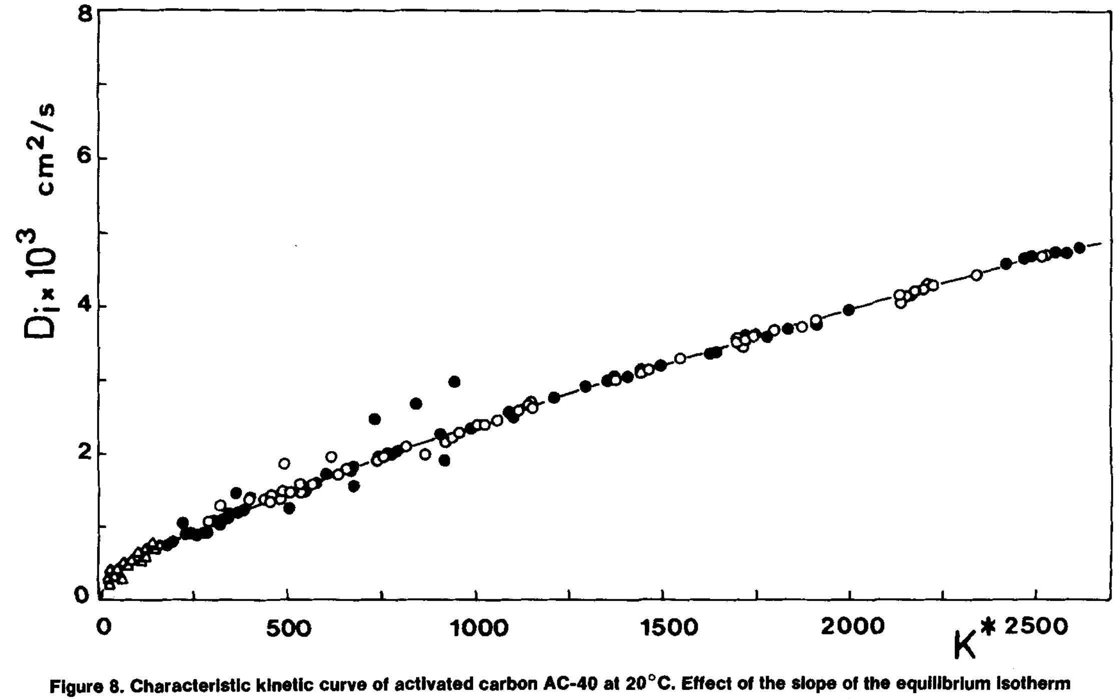

Figure 8. Characteristic kinetic curve of activated carbon AC-40 at 20°C. Effect of the slope of the equilibrium isotherm of each individual hydrocarbon on its respective internal diffusion coefficient (for methane (△), ethane (○) and ethylene (●) as pure components and in their binary and ternary mixtures).

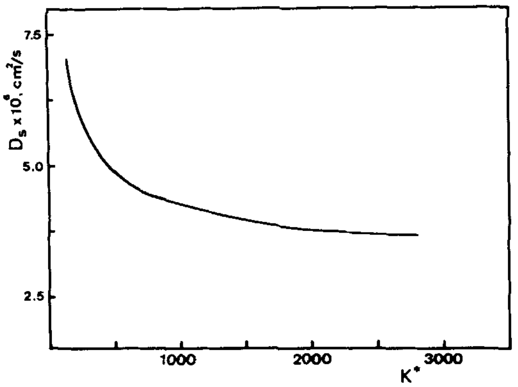

Figure 9. Variation of the surface migration coefficients D_s for each individual hydrocarbon with the slope of the respective adsorption isotherm.

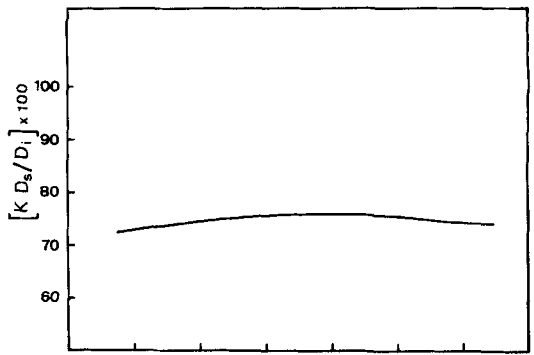

Figure 10. Contribution of the surface migration mechanism to the global mass transfer process inside the adsorbent particles.

SUMMARY

The result that all the values of the internal diffusion coefficient fit into a single characteristic kinetic curve, Figure 8, can be explained primarily by the following facts:

a) Clear predominance of surface migration over diffusion in the gas phase filling the pores of the adsorbent particles, Figure 10.

b) Similarity of the values of the surface migration coefficient of the hydrocarbons investigated for the same range of slopes K.

c) Predominance of the variations of the slopes of the equilibrium isotherms over the variations of the surface migration coefficients themselves, Figure 9.

With much shorter experimentation than that presented in this paper, analogous characteristic kinetic curves could be obtained for other adsorbents.

For adsorbents with a wide range of pore sizes, such as the carbon used here, we believe our curves would be valid for all adsorbable substances with favorable isotherms (Giles, 1960; Hall, 1966). For adsorbents such as molecular sieves, with a uniform pore size, we consider that our curves could be valid only for substances with a *molecular configuration and with an average size that is not critical* with respect to the zeolite pore size. In such cases, the usefulness of our curves is evident: Only the equilibrium isotherms of the substances, pure or in their mixtures, which are easy to obtain experimentally or to predict theoretically from the equilibrium characteristic curve of the adsorbent in the case of pure substances (Myers and Sircar, 1981), would be required to estimate with precision the internal diffusion coefficients of the substances and thus predict their kinetic behavior.

NOTATION

a = empirical parameter in Eq. 15, cm^2/s^2
b = empirical parameter in Eq. 15
c_g = adsorbate concentration in gaseous phase filling pores, mol/cm^3 of pores
c_{g_o} = initial adsorbate concentration in gaseous phase filling pores for $t = 0$, mol/cm^3 of pores
c_s = adsorbate concentration in adsorbed phase, mol/cm^3 of solid
c_{s_o} = initial adsorbate concentration in adsorbed phase for $t = 0$, mol/cm^3 of solid
C = adsorbate concentration in bulk gas surrounding particles, mol/cm^3
C_e = equilibrium concentration in bulk gas surrounding particles, mol/cm^3
C_o = initial adsorbate concentration in bulk gas surrounding particles for $t = 0$, mol/cm^3
C_s = adsorbate concentration in bulk gas phase at particle surface, mol/cm^3
D_g = gas phase diffusion coefficient, cm^2/s
D_i = internal diffusion coefficient, cm^2/s
D_s = surface migration coefficient, cm^2/s
K = $K^* (1 - \alpha_p)/\alpha_p$ (dimensionless)
K^* = slope of adsorption isotherm (moles adsorbed/cm^3 of solid)/(moles of adsorbate/cm^3 of gas)
k_g = mass transfer coefficient for gas phase film around adsorbent particles, cm/s
N = adsorbed moles of adsorbate at equilibrium, mol/g adsorbent
$\overline{N}$ = average adsorbed moles of adsorbate at equilibrium, mol/g adsorbent
P = equilibrium partial pressure of adsorbate, mm Hg (0.133 kPa)
$\overline{P}$ = average equilibrium partial pressure of adsorbate, mm Hg (0.133 kPa)
r = radial position in spherical coordinates, cm
r_o = radius of adsorbent particles assumed to be spherical, cm
R_g = rate of disappearance of adsorbate in gas phase, mol/cm^3·s
R_s = rate of appearance of the adsorbate in the adsorbed phase, mol/cm^3·s of solid
t = time, s
t_e = equilibrium time for adsorption, s
V = gas volume in adsorption bed, cm^3
W = weight of solid particles in the bed, g
Y = dimensionless concentration of adsorbate in bulk gas, Eq. 12
Y_e = equilibrium dimensionless concentration of adsorbate in bulk gas for $C = C_e$, Eq. 12

Greek Letters

α_p = porosity of adsorbent particles
β = parameter defined in Eq. 13
γ = solutions of transcendental Eq. 14
ϵ = parameter defined in Eq. 13
ρ_p = apparent density of adsorbent particles, g/cm^3 of particle
ρ_s = density of solid adsorbent, g/cm^3

APPENDIX

Sample calculation of D_i for an experiment of adsorption (experiment No. 3, corresponding to pure ethane, Table 2):

Calculation of Parameters

Calculation of K^*

From the experimental isotherm of pure ethane:

Initial point

$$P = 1.79 \text{ mm Hg } (238 \text{ Pa}); \quad N = 9.953\ 10^{-5} \text{ mol/g}$$

Final point

$$P = 3.00 \text{ mm Hg } (399 \text{ Pa}); \quad N = 1.472\ 10^{-4} \text{ mol/g}$$

$$K^* = \left(\frac{\Delta N}{\Delta P}\right) RT\rho_s = 2{,}201.28$$

$$\overline{P} = 2.396 \text{ mm Hg } (318.7 \text{ Pa}); \quad \overline{N} = 1.234\ 10^{-4} \text{ mol/g}$$

Calculation of r_o

From Costa et al. (1975):

$$r_o = \frac{3}{2}\left(\frac{r \cdot l}{r + l}\right) = 0.096 \text{ cm}$$

where r_o represents the radius of the sphere with the same ratio of external surface to volume as that of a cylindrical particle of radius r and height l (Table 1).

Determination of D_i

Calculation of $(t_e)_{\text{exp}}$

From the gaseous phase analysis: $(t_e)_{\text{exp}} = 8$ min

Assumed values for D_i (cm^2/s)

$$D_i = 0.009; 0.007; 0.006; 0.005; 0.004; 0.003; 0.002; 0.001$$

Calculated equilibrium times t_e (s) *and concentration for each D_i (Eqs. 12, 13, 14)*

$$t_e = 228; 294; 342; 408; 510; 690; 1{,}020; 2{,}040$$

$$Y_e = 0.071$$

The total number of terms of the series in Eq. 12 required for an accurate calculation of t_e was always smaller than 40.

Calculation of constants a and b

From Eq. 15 and previous values of D_i and t_e:

$$a = 2.03997$$

$$b = -1.00000$$

Calculation of D_i

From values calculated for a, b and $(t_e)_{\text{exp}}$, from Eq. 15:

$$D_i = a(t_e)^b_{\text{exp}} = 0.00425 \text{ cm}^2/\text{s}$$

LITERATURE CITED

Broughton, D. B., "Bulk Separations via Adsorption," *Chem. Eng. Prog.* (Oct. 1977).

Chao, R., and H. E. Hoelscher, "Simultaneous Axial Dispersion and Adsorption in a Packed Bed," *AIChE J.*, **12**, 271 (1966).

Costa, E., and F. Oltra, "Transferencia de Materia en Procesos de Adsorción. Difusión en el Interior del Sólido. II: Resultados," *An. R. Soc. Esp. Fis. Quim.*, **67**, 665 (1971).

Costa, E., et al., "Transferencia de Materia en Procesos de Adsorción. Determinación de los Coeficientes de Difusión en Desorción," *An. R. Soc. Esp. Fis. Quim.*, **71**, 332 (1975).

Costa, E., A. Lucas, and M. E. González, "Ion Exchange. System Amberlite IR-120 $H^+ - Na^+$. Determination of Interdiffusion Coefficients." *Ind. Eng. Chem. Fund.*, **23**, 381 (1984).

Costa, E., J. L. Sotelo, G. Calleja, and C. Marron, "Adsorption of Binary and Ternary Hydrocarbon Gas Mixtures on Activated Carbon: Experimental Determination and Theoretical Prediction of the Ternary Equilibrium Data," *AIChE J.*, **27**, 5 (1981).

Domingo, F., "Adsorption of Light Hydrocarbons and their Mixtures: Determination of Diffusion Coefficients," Ph.D. Thesis (Spanish), Facultad de Ciencias Químicas, Universidad Complutense de Madrid (1981).

Edeskuty, F. J., and N. R. Amundson, "Effect of Intraparticle Diffusion. Agitated Nonflow Adsorption Systems," *Ind. Eng. Chem.*, **44**, 1,698 (1952).

Feng, C. F., and W. E. Stewart, "Practical Models for Isothermal Diffusion and Flow of Gases in Porous Solids," *Ind. Eng. Chem. Fund.*, **12**, 143 (1973).

Feng, C. F., V. V. Kostrov, and W. Stewart, "Multicomponent Diffusion of Gases in Porous Solids. Models and Experiments," *Ind. Eng. Chem. Fund.*, **13**, 5 (1974).

Furusawa, T., and J. M. Smith, "Fluid-Particle and Intraparticle Mass Transport in Slurries," *Ind. Eng. Chem. Fund.*, **12**, 197 (1973).

Gamson, B. W., "Heat and Mass Transfer," *Chem. Eng. Prog.*, **47**, 19 (1951).

Giles, C. H., et al., "Studies in Adsorption. IX: A System of Classification of Solution Adsorption Isotherms and Its Use in Diagnosis of Adsorption Mechanisms and in Measurement of Specific Surface Areas of Solids," *J. Chem. Soc.*, 3,973 (1960).

Gilliland, E. R., R. F. Baddour, and J. L. Russell, "Rates of Flow Through Microporous Solids," *AIChE J.*, **4**, 90 (1958).

Gilliland, E. R., et al., "Diffusion on Surfaces. I: Effect of Concentration on the Diffusivity of Physically Adsorbed Gases," *Ind. Eng. Chem. Fund.*, **13**(2), 95 (1974).

Hall, K. R., et al., "Pore and Solid Diffusion Kinetics in Fixed-Bed Adsorption under Constant Pattern Conditions," *Ind. Eng. Chem. Fund.*, **5**, 212 (1966).

Kokoszka, J. J., "Multicomponent Rates of Sorption of Propane and Butane from Helium by 5A Molecular Sieve Sorbent," M.S. Thesis, Worcester (Mass.) Polytech. Inst. (1970).

Lee, H., and T. W. Weber, "Isothermal Adsorption in Fixed Beds," *Can. J. Chem. Eng.*, **47**, 54 (1969).

Lee, H., and C. W. Chi, "Carbon Dioxide Removal from Air by Sodium-X Molecular Sieve Under Nonisothermal Conditions," *AIChE Symp. Ser. 117*, **67**, 84 (1971).

Lewis, W. K., E. R. Gilliland, and W. P. Cadogan, "Adsorption Equilibria Hydrocarbon Gas Mixtures," *Ind. Eng. Chem.*, **42**, 1,319 (1950).

Ma, Y. H., and A. J. Roux, "Multicomponent Rates of Sorption of SO_2 and CO_2 in Sodium Mordenite," *AIChE J.*, **19**, 1,055 (1973).

Ma, Y. H., and T. Y. Lee, "Diffusion of Binary Gas Mixtures in Zeolite X Pellets," *Ind. Eng. Chem. Fund.*, **16**, 44 (1977).

Marcussen, L., "The Kinetics of Water Adsorption on Porous Alumina," *Chem. Eng. Sci.*, **25**, 1,487 (1970).

Masamune, S., and J. M. Smith, "Adsorption Rate Studies—Significance of Pore Diffusion," *AIChE J.*, **10**, 246 (1964).

Meyer, O. A., and T. W. Weber, "Nonisothermal Adsorption in Fixed Beds," *AIChE J.*, **13**, 457 (1967).

Milton, R. M., "Hydrocarbon Separation," U.S. Patent 3,078,645 (1963).

Myers, A. L., and J. M. Prausnitz, "Thermodynamics of Mixed Gas Adsorption," *AIChE J.*, **11**, 121 (1965).

Myers, A. L., and S. Sircar, "Characteristic Adsorption Isotherm for Adsorption of Vapors on Heterogeneous Adsorbents," Publication pending, *AIChE J.*

Nemeth, E. J., and E. B. Stuart, "Pore-Diffusion Mechanisms during Vapor-Phase Adsorption," *AIChE J.*, **16**, 999 (1970).

Ponzi, H., et al., "On the Surface Diffusion of Adsorbable Gases Through Porous Media," *AIChE J.*, **23**, 347 (1977).

Priegnitz, J. W., "The Selective Separation of Butene-1 from a C_4 Hydrocarbon Mixture Employing Zeolites X and Y," U.S. Patent 3,723,561 (1973).

Schneider, P., and J. M. Smith, "Chromatographic Study of Surface Diffusion," *AIChE J.*, **14**, 886 (1968).

Sladek, K. J., E. R. Gilliland, and A. F. Baddour, "Diffusion Surfaces. II: Correlation of Diffusivities of Physically and Chemically Adsorbed Species," **13**, 100 (1974).

Smith, J. M., *Chemical Engineering Kinetics*, 3rd ed., McGraw-Hill, New York (1981).

Sudo, Y., D. M. Misic, and M. Suzuki, "Concentration Dependence of Effective Surface Diffusion Coefficients in Aqueous Phase Adsorption on Activated Carbon," *Chem. Eng. Sci.*, **33**, 1,290 (1978).

Yatsurugi, Y., "Process for Preparing 4 and 5A Zeolite and Method for Separating Mixtures Using the Same," U.S. Patent 3,785,122 (1974).

Manuscript received Apr. 30, 1982; revision Apr. 17, 1984, and accepted Apr. 30.